

COGEAR

MODULE 3:

Geotechnical measurements in the Matter valley

Del. No.: 3b.2.2

**Authors: Moore, J., Yugsi, F., Gischig, V.,
Button, E., and Löw, S.**

Engineering Geology, ETH Zürich

February 23, 2010

Task 3b.2.2

Geotechnical measurements in the Matter valley

Deliverable: 3b.2.2.1

Jeffrey Moore, Freddy Yugsi Molina, Valentin Gischig, Edward Button, and Simon Loew
Engineering Geology, ETH Zurich

Summary

This report summarizes geotechnical deformation measurements performed at rock slope instabilities the Matter valley undertaken, aided, or acquired by the Engineering Geology group at ETH Zurich. Instability sites described include those at Randa, Medji, Graechen, Walkerschmatt, and Sibulbodme (Figure 1), with a related site - Moosgufer - in the adjacent Saas valley also included. Remote displacement monitoring methods include traditional geodetic distance measurement, advanced small-scale geodetic networks, precision differential GPS location, and the latest techniques of satellite- and ground-based radar interferometry. In-situ displacement monitoring methods range from basic hand measurements of crack opening, to borehole surveys, to the latest high-resolution techniques based on fiber optic strain sensors.

Randa

Since 2001, the Engineering Geology group at ETH Zurich has maintained an 'in-situ laboratory' at the rock slope instability located above the town of Randa in the Matter valley (46.113116° , 7.774713°). The slope failed catastrophically in 1991, releasing around 30 million m^3 of crystalline rock (Figure 2). Currently, we estimate that around 5-7 million m^3 of material remains unstable, moving towards the valley at up to 20 mm/yr (Gischig et al., 2009). Geotechnical measurements aim to describe the key structures controlling rock mass deformation, derive kinematic modes of displacement, and elucidate those mechanisms driving progressive failure.

Remote measurements

Large-scale geodetic network

In 1995, a geodetic network, consisting of seven 3D reflectors and eighteen 1D reflectors located in the crown and along the edge of the scarp, was setup to monitor rock mass displacements at Randa (Figure 3). Since 1996, the displacement of the seven 3D retro-reflectors was measured by surveying a geodetic network with a total station once or twice per year (Willenberg et al., 2008b). The 18 1-D points were surveyed using a total station positioned on a monument on the opposite valley wall. Figure 6 shows the time series for both geodetic measurements and GB-DInSAR (described later), as well as the locations of these points on an unwrapped (i.e. phase wrapping removed) GB-DInSAR displacement map of 248 days interval. The error bars are 2.5 mm for the geodetic measurements and 1 mm for each GB-DInSAR repeat measurement.

Small-scale geodetic network

In September 2008, a small-scale, local geodetic network was installed at the top of the Randa instability (Figure 4). It consists of 35 Leica mini-prisms located in both unstable and stable areas of the rock mass. The stable measurement points serve as reference

points for the presumably unstable points. Distances and angles are measured with a Leica total station (TPS 1201). Small base-lengths of maximum 200 m result in an accuracy of less than 2 mm. The network was surveyed monthly for throughout the course of one year; with the aim to not only obtain highly accurate displacement vectors of individual blocks, but also to reveal any seasonal changes in the displacement rate.

Ground-based DInSAR

Five ground-based differential interferometric synthetic aperture radar (GB-DInSAR) surveys were conducted between 2005 and 2007 at the Randa rock slope instability. GB-DInSAR measurements were conducted by Ellegi Srl (Milano, Italy) using their GB-DInSAR system *LiSA*. The *LiSA* base station was located at 1560 m.a.s.l. on the valley wall opposite the 1991 failure scarp. The system works at a frequency range of 17.1–17.18 GHz. The radar antennas are translated along a 2.7 m long rail in order to create a synthetic aperture. The target distance is 1.3 to 2 km. Azimuth resolution is 4 m in the near range and 6.5 in the far range, range resolution is 1.9 m. Complete system specifications and acquisition parameters for these radar surveys, as well as a full discussion of the results is presented by Gischig et al., (2009). Overview results are presented in Figures 5 and 6.

In-situ measurements

Manual crack measurements

A number of actively opening or suspicious fractures on the ground surface behind the crown of the currently unstable rock mass have been mapped, and key locations selected for long-term monitoring. Manual measurements of crack width have been made at eighteen cracks since at least 2001. These cracks are either measured by simple benchmark measurements perpendicular to the crack using a tape measure or more precise caliper gauge (± 0.1 mm), or with benchmark quadrilateral arrays that allow the different components of the displacement vector to be resolved. Figure 7 shows a summary of the results, indicating long-term opening rates.

Inclinometer surveys

Each of the three boreholes at Randa (sb50n, sb50s, and sb120) is equipped with grooved PVC inclinometer casing (Figure 8). Periodic inclinometer surveys were performed twice per year from 2002 through 2006, and more sparsely thereafter. All inclinometer surveys used a 61 cm base length, bi-axial instrument. Results for borehole sb120 are presented in Figure 9, and have been used to identify actively deforming faults and fracture zones along the borehole axis, and to characterize their rates of displacement. Detailed description of the measurement system and full results can be found in Willenberg et al. (2008b).

Extensometer surveys

The deepest borehole (sb120) has also been fitted with external brass rings at 1 m intervals for extensometer surveying using the INCREX system. The sensor base length (and measurement interval) is 60 cm. Repeat surveys were conducted in conjunction with inclinometer measurements twice per year. Latest results are shown in Figure 9, and are used to help characterize actively deforming fractures and axial displacement rates in the borehole. Detailed description of the measurement system and full results can be found in Willenberg et al. (2008b).

Borehole inclinometers

Two in-place inclinometers (Vibrating Wire, Model 6300 from Geokon) are installed across discontinuities in the deep boreholes at Randa. Their purpose is to monitor continuous displacements across these discontinuities and to detect temporal changes in

the displacement rate. The instruments measure changes in tilt, which allows for computing the horizontal displacement using the base length of the instrument (1.87 m). The inclinometers have been operational since January 2004. Between 2004 and 2008 they were placed at 68 m and 85 m depth in the sb120 borehole. These locations were chosen according to periodic inclinometer surveys, which showed significant displacement across discontinuities at those depths (see Figure 9). The sampling interval in this time period is 1 hour. Detailed description of the measurement system and results can be found in Willenberg et al. (2008a,b), and example results are shown in Figure 10.

Crack extensometers

Two Vibrating Wire crack extensometers ("crackmeters" - Geokon model 4420) continuously measure opening of two monitored tension cracks at the ground surface (cracks q2 and x2 (also called Z9 and Z10); Figure 8). These sensors have been operational since January 2003 and run at a sampling rate of 1 hour (before August 2008) and 30 min (since August 2008). Resolution is 0.03 mm with a reported accuracy of 0.15 mm. A thermistor is built into each sensor for thermal strain compensation. Both cracks show a strong seasonal pattern of deformation with closure during warming periods and opening during cooler periods. Example data are shown in Figure 11. Detailed description of the measurement system and results can be found in Willenberg et al. (2008b).

Fiber optic strain sensors

To improve and extend the monitoring strategy at Randa, with the added goal of understanding the seismic response of the rockslide, a fiber optic strain monitoring system was installed in summer 2008 based on long-gage Fiber Bragg Grating sensors. The new monitoring system can detect sub-micrometer scale deformations in both triggered-dynamic and continuous measurements. Two types of sensors have been installed: (1) fully embedded borehole sensors and (2) surface extensometers. Dynamic measurements are triggered by sensor deformation and recorded at 100 Hz, while continuous data are logged every 5 minutes. Resolution varies with the sensor base length but is around 0.5 μm on average, while the long-term accuracy is about 2 μm . The full system specifications and description of monitoring results to-date can be found in Moore et al. (2010), while example time series data are shown in Figures 12 and 13.

Medji

The Medji rockslide occurred on the evening of November 21, 2002 above the village of St. Niklaus (46.167414°, 7.787053°). In total, 70,000 m³ of rock collapsed from an unstable nose in highly-dissected, steep terrain (Figures 14 and 15). Since 2002, various instabilities remain in the immediate vicinity, controlled by large-scale tectonic faults and fracture zones.

In-situ and remote deformation measurements

Deformation measurements made in support of hazard assessment prior to the 2002 rockslide are summarized in a report from the responsible geological consultants Rovina + Partner, AG. The relevant figures will not be reproduced here. Measurements performed include crack extension time series at multiple locations, borehole tilt, and geodetic distance measurement. Accelerations noted in the time series were used to help reveal impending failure and alert local authorities to order evacuation of endangered settlements.

Satellite InSAR

Interferometric Synthetic Aperture Radar (InSAR) displacement images created using interferometric point target analysis (IPTA) were acquired with support from the ESA (European Space Agency) in the framework of the SLAM (Service for Landslide Monitoring) project of the Swiss Federal Office for the Environment (Farina et al., 2006). Results reveal clear indications of ongoing movements within the regions adjacent to the 2002 failure (Figure 16). Especially the area above and behind the 2002 detachment zone stands out as moving at rates of 15 mm/yr and higher.

Ground-Based DInSAR

Two ground-based differential interferometric synthetic aperture radar (GB-DInSAR) surveys were conducted between September and November, 2005 at the Medji rock slope instability. GB-DInSAR measurements were conducted by Ellegi Srl (Milano, Italy) using their *LiSA* system. Measurements were made from a point located on the valley wall opposite the 2002 failure, about 1500 m distant. The system operates at a frequency range of 17.1–17.18 GHz, and the radar antennas are translated along a 2.7 m long rail in order to create a synthetic aperture. Azimuth resolution was 3.3 m in the near range and 6.2 m in the far range, range resolution is 1.9 m. Summary results are presented in LiSALab (2005) and reveal zones of continued ongoing movement in the area surrounding the 2002 failure. Full results and system specifications can be found in LiSALab (2005) and will not be reproduced here.

Graechen

Graechen is a very large deep seated gravitational slope deformation (DSGSD) located on the eastern flank of the Matter valley near its confluence with the Saas valley (Figure 17). The town of Graechen sits on a flat bench at around 1600 m a.s.l. in the middle section of the DSGSD. Above the town, steep slopes rise up broken rocky terrain to high peaks in permafrost terrain. Numerous rock slope instabilities exist at all scales within the Graechen area, which requires use of a broad range of monitoring techniques.

Long-term geodetic measurements

Displacements of nine fixed measurement points have been monitored over an interval of 62 years as part of a long-term study. Full results and measurement details are described by Noverraz et al. (1998). The results reveal the first conclusive indication that large mass of the suspected DSGSD at Graechen is currently moving at appreciable rates. Movement rates up to 8 mm/yr were measured, and their distribution helps estimate the limits of the unstable mass (Figure 18). Unfortunately, a denser array of measurement points is not available, and the lateral extents of the DSGSD remain poorly constrained in some areas.

Satellite InSAR

Interferometric Synthetic Aperture Radar (InSAR) displacement images created using interferometric point target analysis (IPTA) were acquired with support from the ESA (European Space Agency) in the framework of the SLAM (Service for Landslide Monitoring) project of the Swiss Federal Office for the Environment (Farina et al., 2006).

The area of Graechen was selected for detailed analysis and reporting, and the measurement procedure and displacements revealed through InSAR monitoring are described in the SLAM monographic report: Grächen, Montagnon & La Frasse (2004). Select results showing measured displacements are reproduced in Figures 19 and 20. Movement rates on the order of 3 mm/yr (along LOS) can be deduced for the large flat region in the central portion of the DSGSD around the town of Graechen. The data can be used to better delineate the extents of the DSGSD and to identify areas of increased movement and local instabilities.

Detail study sites – Durlochhorn, Gabelhorn, and Platja

Select sites within the Graechen area have been chosen for detailed analysis (Figure 21). Rock slopes on the Durlochhorn and Gabelhorn (near the Seetalhorn lift station) have been selected for time-lapse photography and LiDAR difference surveys as part of a new project regarding rock slope sensitivity (K. Leith). First measurements have been accomplished, with repeat measurements to follow 3-4 times per year. At Platja (Figure 22), a network of large rock blocks separated by wide tension cracks has been investigated as part of an ongoing M.Sc. thesis project (M. Heynen). The crack network and relative displacements are described, and infrastructure for in-situ displacement measurements using a tape extensometer has been installed. Baseline measurements of crack opening were made in 2009, with follow up surveys scheduled for 2010.

Walkerschmatt

Walkerschmatt is a large suspected rock slope instability located at 2080 m a.s.l. above the village of Biffig on the western flank of the Matter valley (46.162357°, 7.779824°). An overview of the area is shown in Figure 23. Numerous open cracks can be found traversing a small alp on the shoulder high above the main inner valley. Precision differential GPS measurements were not conclusive, but suggest the site is either currently not moving or moving at rates below resolution limits, which is also supported by regional geodetic monitoring (pers. comm. K. Aufdenblatten). The volume of the instability has been estimated at around 600,000 m³.

Differential GPS measurements

High-precision differential GPS measurements were performed in September 2008 and June 2009 at a number of fixed points located within the suspected instability. Measurements were conducted in cooperation with the Institute of Geodesy and Photogrammetry at ETH Zurich (Ingensand and Stempfhuber, 2009). Differential GNSS measurements were used to determine the precise location of each fixed point, and tied to the Swiss national network for absolute coordinates. The resulting locations were then differenced to reveal any displacement of the fixed points over the 10 month period. Displacements greater than 5 mm in the horizontal and 8 mm in the vertical direction are considered statistically significant. Five fixed points were surveyed in the Walkerschmatt area and the results are summarized in Figure 24. Of these, two points (smaller arrows) showed displacements below the computed accuracy level so are not considered significant. The remaining three points were only slightly above the accuracy threshold, so their results should be analyzed with caution. The orientations of resolved GPS displacements are in good internal agreement, but these differ from field observations of crack opening directions by more than 90 degrees in some cases. Therefore, these results are considered somewhat inconclusive.

Satellite InSAR

Interferometric Synthetic Aperture Radar (InSAR) displacement images created using interferometric point target analysis (IPTA) were acquired with support from the ESA (European Space Agency) in the framework of the SLAM (Service for Landslide Monitoring) project of the Swiss Federal Office for the Environment (Farina et al., 2006). Resulting displacement data in the Walkerschmatt area do not reveal conclusive movements as there are very few IPTA reflectors located within or near the suspected unstable rock mass.

Sibulbodme

Sibulbodme is an apparently active slope instability located at 2450 m a.s.l. on the western flank of the Matter valley above the village of Mattsand (46.148931°, 7.772890°). An overview of the area is shown in Figure 25. Large-scale faults and fracture zones delineate an estimated 225,000 m³ of unstable rock. Differential GPS measurements and satellite IPTA data confirm that the rock slope is currently unstable.

Differential GPS measurements

High-precision differential GPS measurements were performed in September 2008 and June 2009 at a number of fixed points located within the suspected instability. Measurements were conducted in cooperation with the Institute of Geodesy and Photogrammetry at ETH Zurich (Ingensand and Stempfhuber, 2009). Differential GNSS measurements were used to determine the precise location of each fixed point, and tied to the Swiss national network for absolute coordinates. The resulting locations were then differenced to reveal any displacement of the fixed points over the 10 month period. Displacements greater than 5 mm in the horizontal and 8 mm in the vertical direction are considered statistically significant. Five fixed points were surveyed in the Sibulbodme area by static methods, with an additional thirteen points added using a local reference station (RTK-LRS) by rapid-static methods. The results are summarized in Figure 26. Of the measured values, all points on the local network (blue arrows) were found to be above the accuracy threshold and show consistent displacement directions in agreement with field observations. Therefore, these results are considered significant. Measured displacements are on the order of 15 mm over the ~1 year period, and show block movement to the northeast. Measurements were made behind the active area to investigate the presence of a larger instability, however these were inconclusive.

Satellite InSAR

Interferometric Synthetic Aperture Radar (InSAR) displacement images created using interferometric point target analysis (IPTA) were acquired with support from the ESA (European Space Agency) in the framework of the SLAM (Service for Landslide Monitoring) project of the Swiss Federal Office for the Environment (Farina et al., 2006). Resulting reflector data are sparse in the Sibulbodme area, but indicate areas of movement at rates up to 1.5 mm/yr. Particularly the area of the north facing slope covered with talus blocks (see Figure 25) shows indications of movement. The results cannot be interpreted further as the IPTA reflectors are too sparse, and there are no reflectors coinciding with the GPS fixed points.

Moosgufer

The Moosgufer rock slope failure and current instability (46.105565° , 7.962157°) is located on the eastern flank of the Saas valley above the town of Saas Amagell. During the course of his investigation, Ruppen (2009) analyzed satellite IPTA data and installed wire line extensometer arrays to constrain active deformations in the head scarp of the pre-historical failure.

In-situ crack measurements

Three wire line extensometer arrays were installed along the head scarp of the pre-historic rock slope failure. Figure 27 provides an overview of the site location and the position of the three arrays denoted MS-Nord, MS-Mitte, and MS-Sud (Ruppen, 2009). Each location is composed of multiple quadrilateral extensometer arrays spanning open fractures which separate individual blocks, and is tied to presumably stable ground with linear extensometer measurements. A full description of each system is available in Ruppen (2009) and will not be reproduced here. The initial measurement of MS-Sud array was on the October 15th 2008, while the other two arrays were measured on the October 21st 2008. No repeat measurements currently exist for these arrays.

Satellite InSAR

Interferometric Synthetic Aperture Radar (InSAR) displacement images created using interferometric point target analysis (IPTA) were acquired with support from the ESA (European Space Agency) in the framework of the SLAM (Service for Landslide Monitoring) project of the Swiss Federal Office for the Environment (Farina et al., 2006). Figure 28 shows the reflector data in the region of the Moosgufer (Ruppen, 2009). These data show that the debris associated with pre-historic failures moves at appreciable rates between 2 mm/yr and 27 mm/yr, with distinct zones (or lobes) moving at similar rates. In the area surrounding the head scarp no IPTA reflectors are observed. To the north of the failure several reflectors are observed that indicate no movement or slight heave, and therefore are not considered to be associated with active slope deformations.

References

- Farina, P., Colombo, D., Fumagalli, A., Marks, F. & Moretti, S. (2006). Permanent Scatterers for landslide investigations: outcomes from the ESA-SLAM project, *Engineering Geology*, 88, 200-217.
- Gischig, V., Loew, S., Kos, A., Moore, J.R., Raetzo, H., and Lemy, F. (2009). Identification of active release planes using ground-based differential InSAR at the Randa rock slope instability, Switzerland, *Natural Hazards and Earth System Sciences* 9(6), 2027-2038.
- Ingensand, H. and Stempfhuber, W. (2009). Überwachungen Rutschhang Mattertal Technischer Bericht Geodätischer Projektkurs 2009 Randa. Institute of Geodesy and Photogrammetry, Swiss Federal Institute of Technology, Zurich.
- Jörg, T. (2008). Versagensmechanismus und Disposition des Medji Felssturz (Mattertal, Wallis), M.Sc. Thesis in Engineering Geology, ETH Zurich.
- LiSALab (2005). Final report: ASTRA project. Contract # 0010050101bwg for Bundesamt Für Umwelt (BAFU).
- Moore, J.R., Gischig, V., Button, E., and Loew, S. (2010). Rockslide deformation monitoring with fiber optic strain sensors, *Natural Hazards and Earth System Sciences* 10(2), 191-201.
- Noverraz, F. et al. (1998). Grands glissements de versants et climat VERSINCLIM- Comportement passé, présent et futur des grands versants instables subactifs en fonction de l'évolution climatique, et évolution en continu des mouvements en profondeur. Ecole Polytechnique de Lausanne, Lausanne, Switzerland.
- Rovina + Partner, Büro für Ingenieurgeologie, 3953 Varen (2005); St.Niklaus, Wallis: „Unneri Spssplatte“, Felsrutschung und Felssturz vom 21.11.2002. Unveröffentlicher Bericht.
- Ruppen, M. (2009). Geologische Charakterisierung und Untersucchung der Haninstabilität im Moosgufer in Saas Almagell (Wallis, Schweiz). M.Sc. Thesis Engineering Geology, ETH Zurich, Switzerland.
- SLAM monographic report: Grächen, Montagnon & La Frasse (2004). Authors: K. Graf and T. Strozzi, project coordinator P. Manunta. Document reference pkt108-251-1.0.
- Willenberg, H. (2004). Geologic and kinematic model of a complex landslide in crystalline rock (Randa, Switzerland). D.Sc. Thesis, Engineering Geology, ETH Zurich, Switzerland.
- Willenberg, H., Loew, S., Eberhardt, E., Evans, K., Spillmann, T., Heincke, B., Maurer, H-R., and Green, A. (2008a). Internal structure and deformation of an unstable crystalline rock mass above Randa (Switzerland): Part I – Internal structure from integrated geological and geophysical investigations, *Engineering Geology* 101, 1-14.
- Willenberg, H., Evans, K.F., Eberhardt, E., Spillmann, T., and Loew, S., (2008b). Internal structure and deformation of an unstable crystalline rock mass above Randa (Switzerland): Part II – Three-dimensional deformation patterns, *Engineering Geology* 101, 15-32.
- <http://www.rockslide.ethz.ch/>

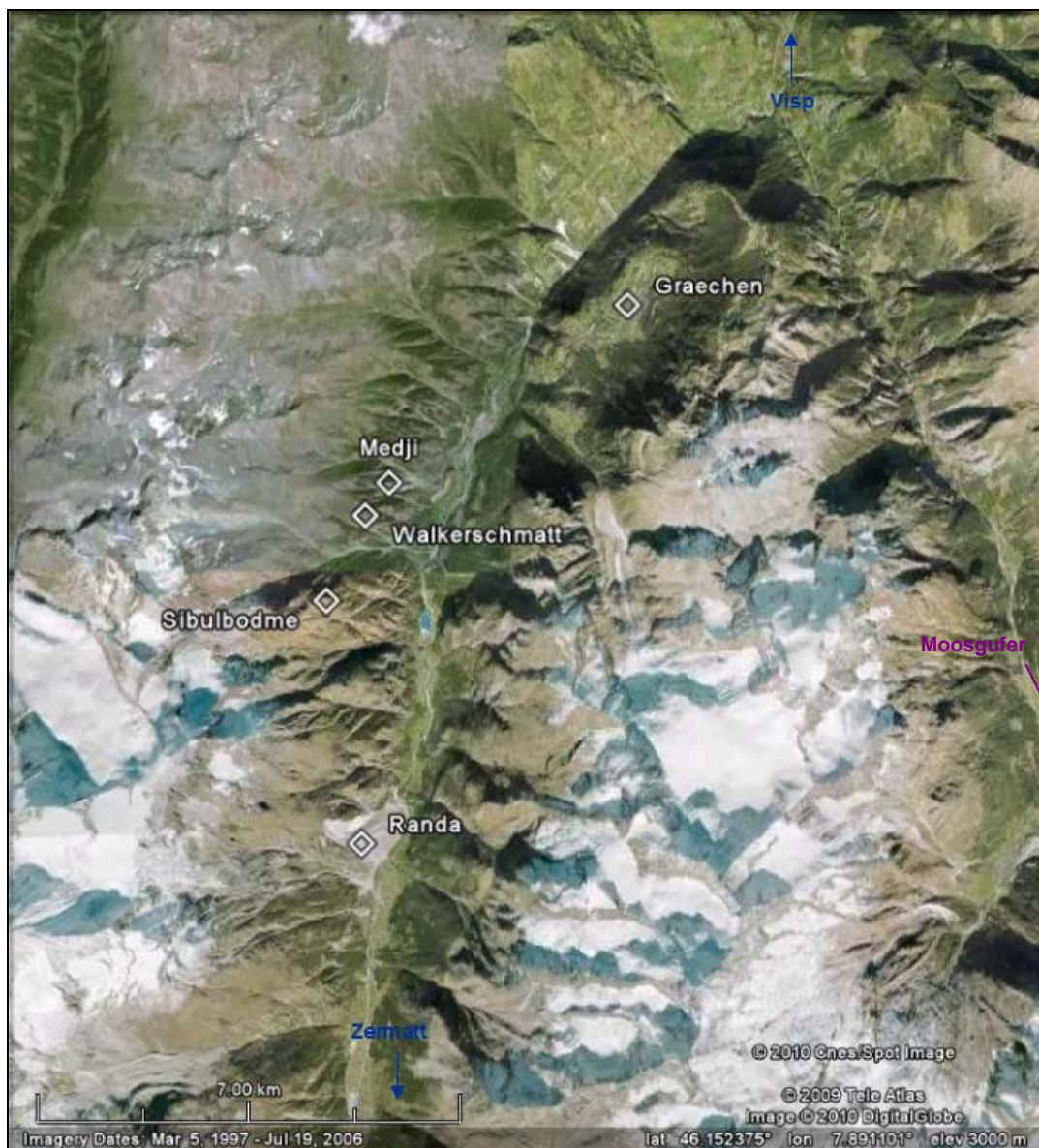


Figure 1: Overview of the study area in the Matter valley, VS. The five detail study sites described in this report are highlighted: Graechen, Medji, Walkerschmatt, Sibulbodme, and Randa, while an additional site – Moosgufer – in the Saas Valley is also described.



Figure 2: Photograph of the Randa rock slope instability showing the talus deposited during the 1991 failures over the town of Randa, VS.

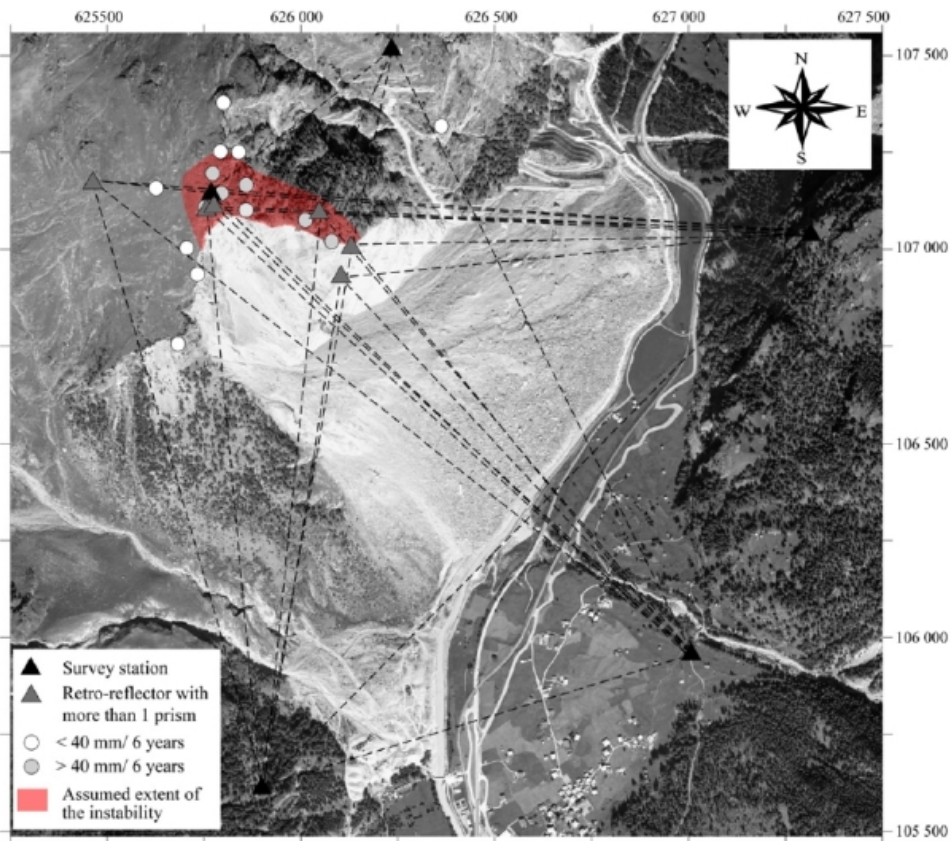


Figure 3: Large-scale geodetic network at Randa showing measuring points and base station location.

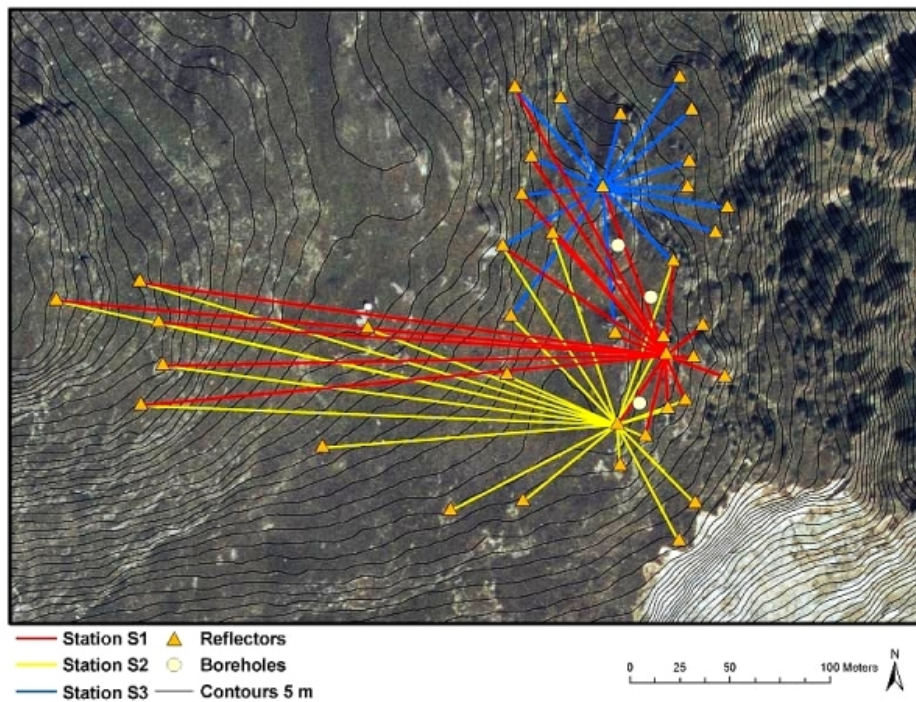


Figure 4: Small-scale (local) geodetic network at Randa showing measurement points and three base stations.

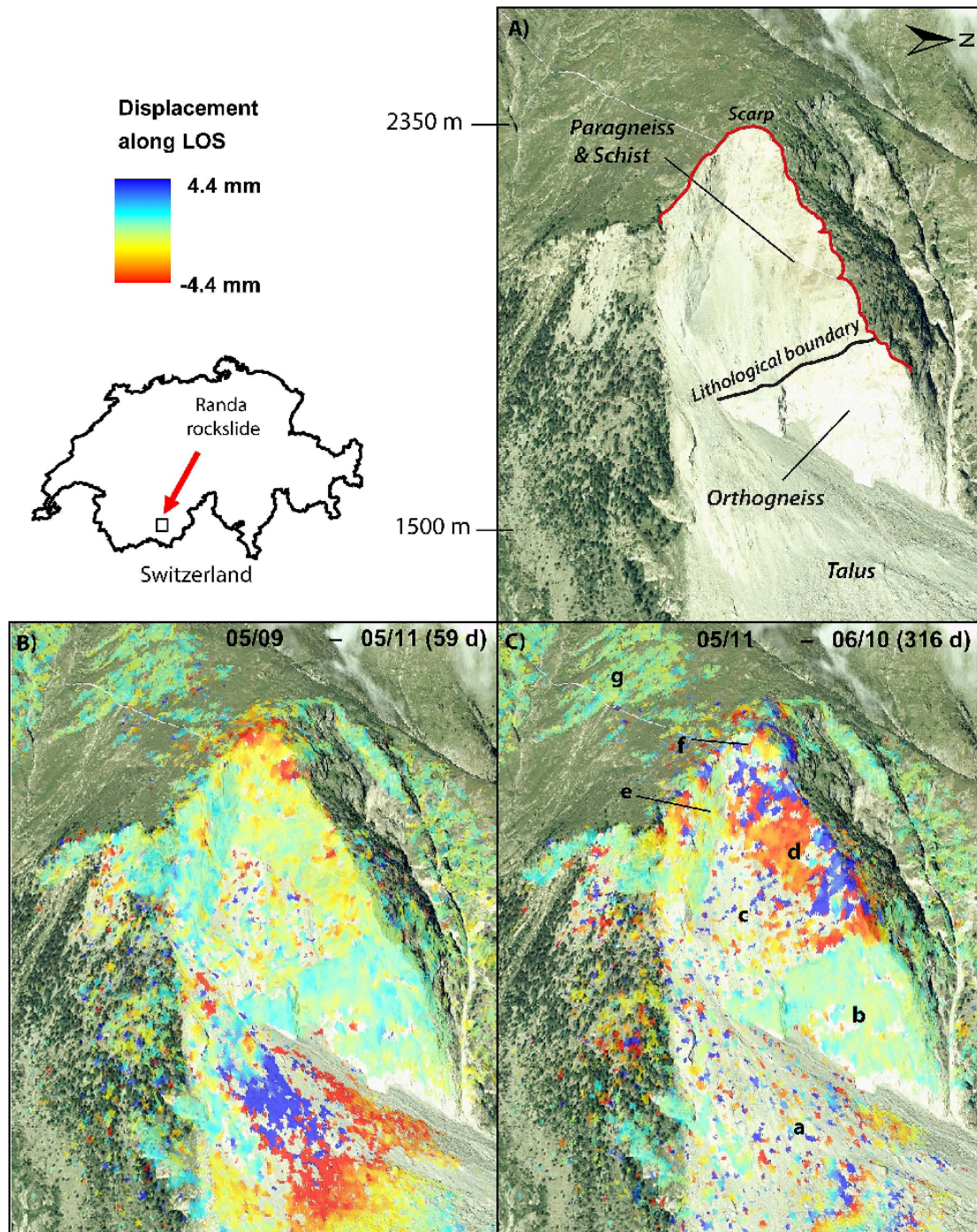


Figure 5: Randa GB-DInSAR data draped onto a DTM with orthophoto. Displacement maps are derived from the 1st repeat with respect to the reference survey (B), as well as from the 2nd with respect to the 1st repeat survey (C). Dates (yy/mm) of the surveys, as well as the number of days between successive surveys are shown. For a full discussion see Gischig et al., 2009.

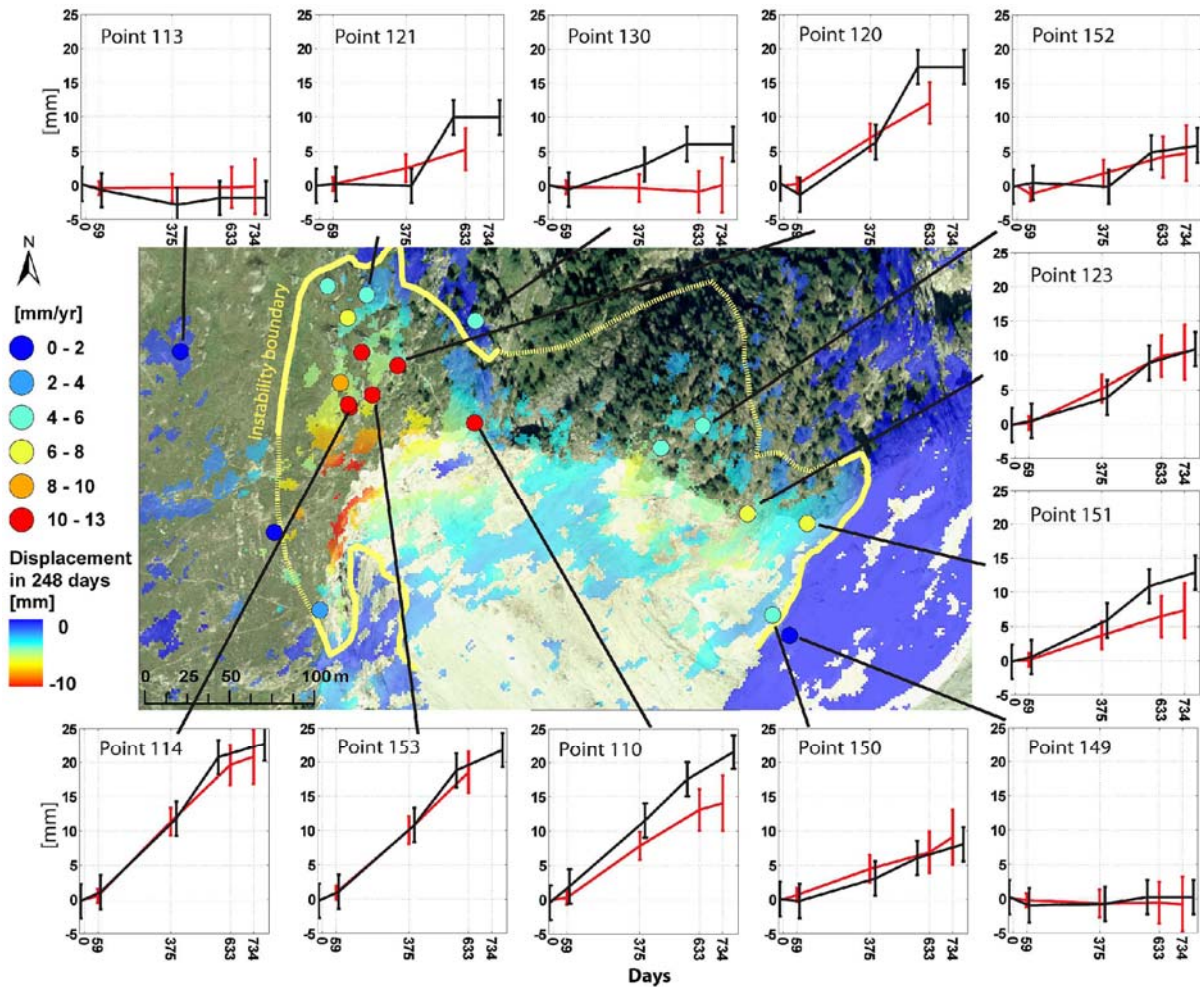


Figure 6: Comparison of geodetic distance measurements with GB-DInSAR displacements at Randa. Time series derived from GB-DInSAR data at the locations of the reflectors are shown in red, geodetic time series are shown in black. Locations of the reflectors are displayed together with an unwrapped displacement map between the 3rd and the 2nd repeat survey (248 days). The yellow line shows the boundary of the instability derived from GB-DInSAR; dashed portions are uncertain. Figure reproduced from Gischig et al., 2009.

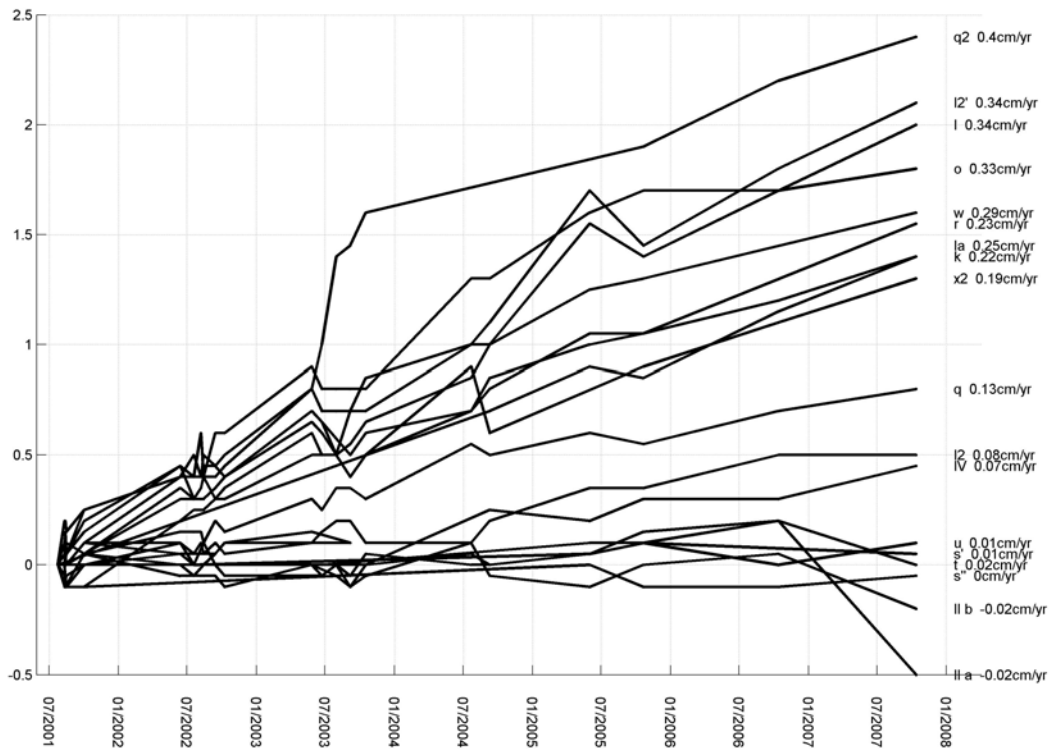


Figure 7: Hand-measured crack opening values at Randa. Crack labels and derived rates are shown.

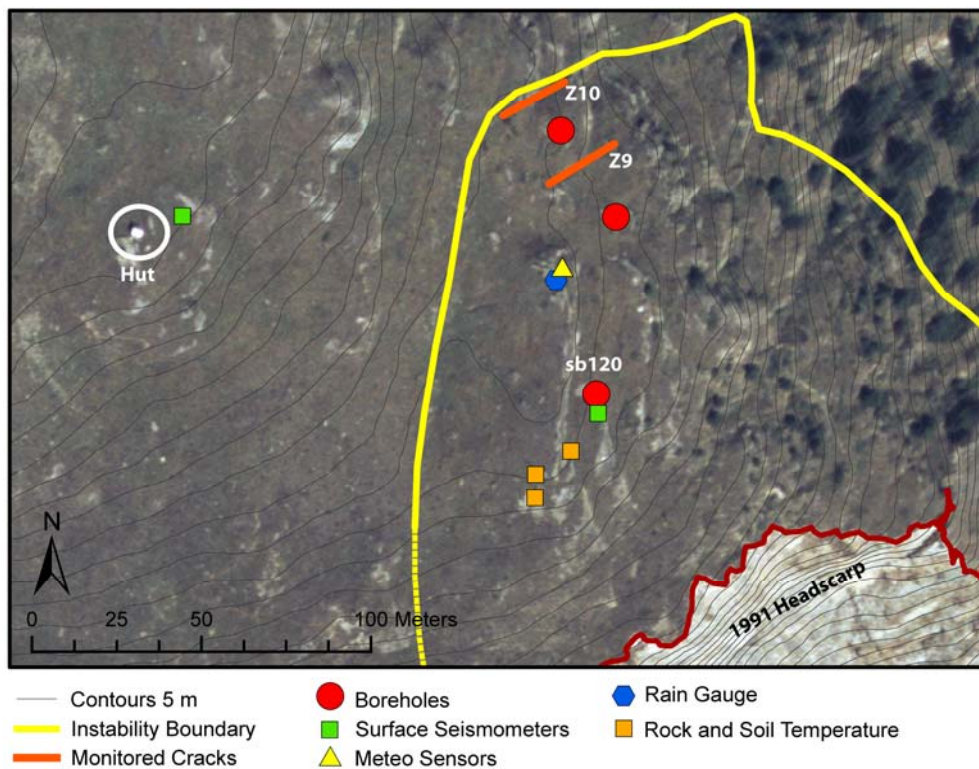


Figure 8: Overview of selected in-situ measurement systems at the Randa instability.

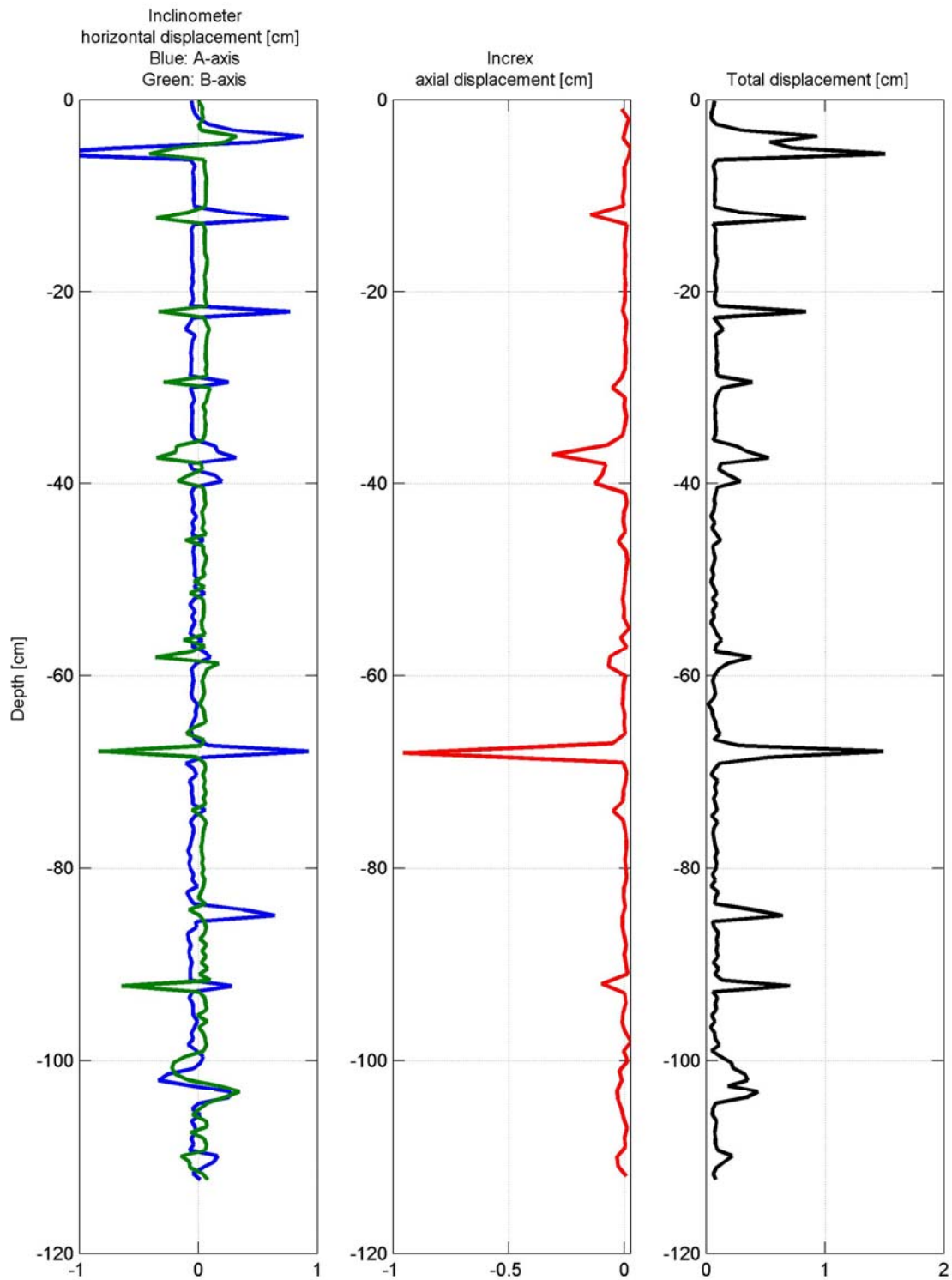


Figure 9: Inclinerometer and extensometer survey results from borehole sb120 at Randa.

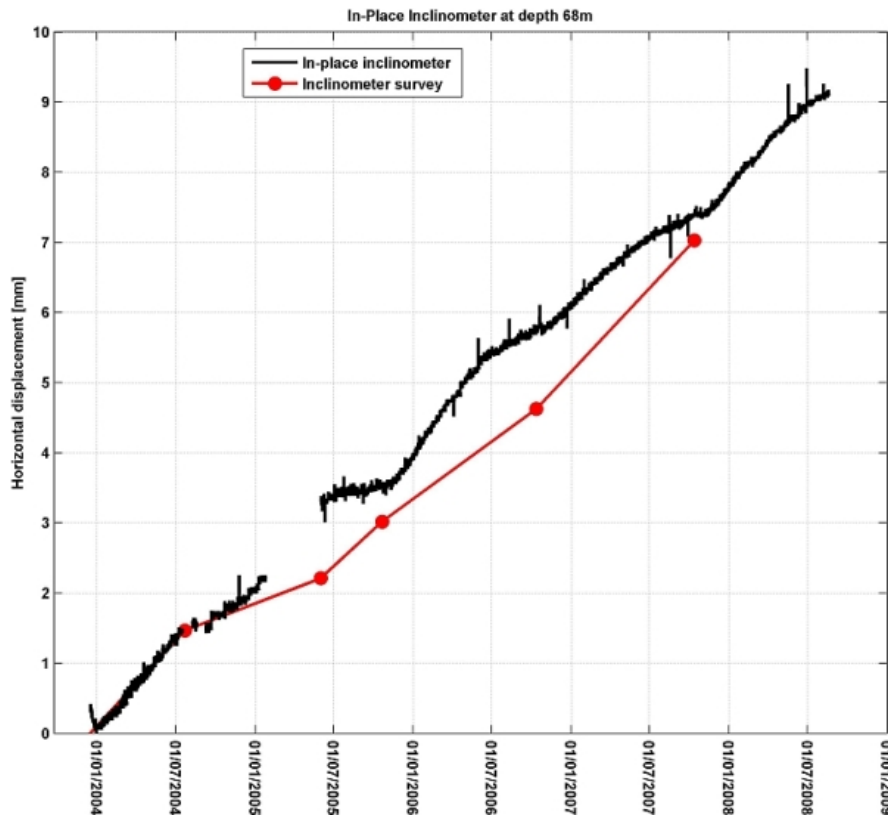


Figure 10: Time series of in-place inclinometer data from Randa borehole sb120. Red line shows the results of periodic inclinometer surveys for comparison.

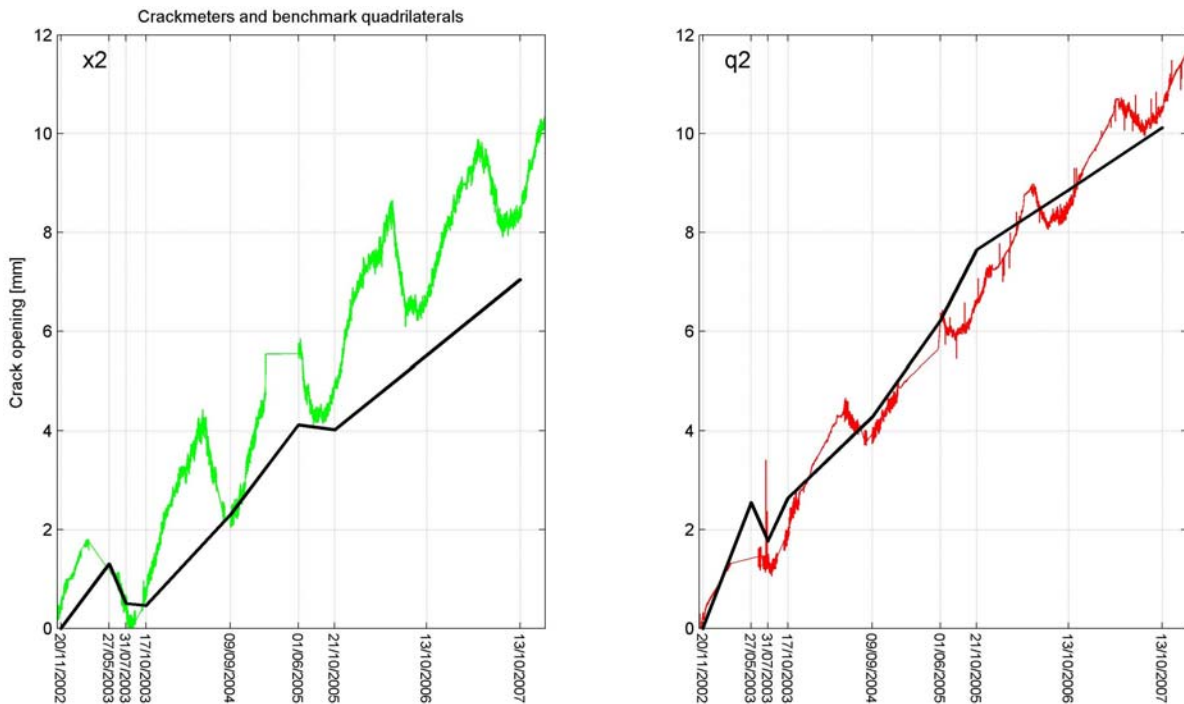


Figure 11: Crack extensometer time series data shown with hand measurements of the benchmark quadrilateral arrays for two cracks (q2 = Z9 and x2 = Z10) at Randa.

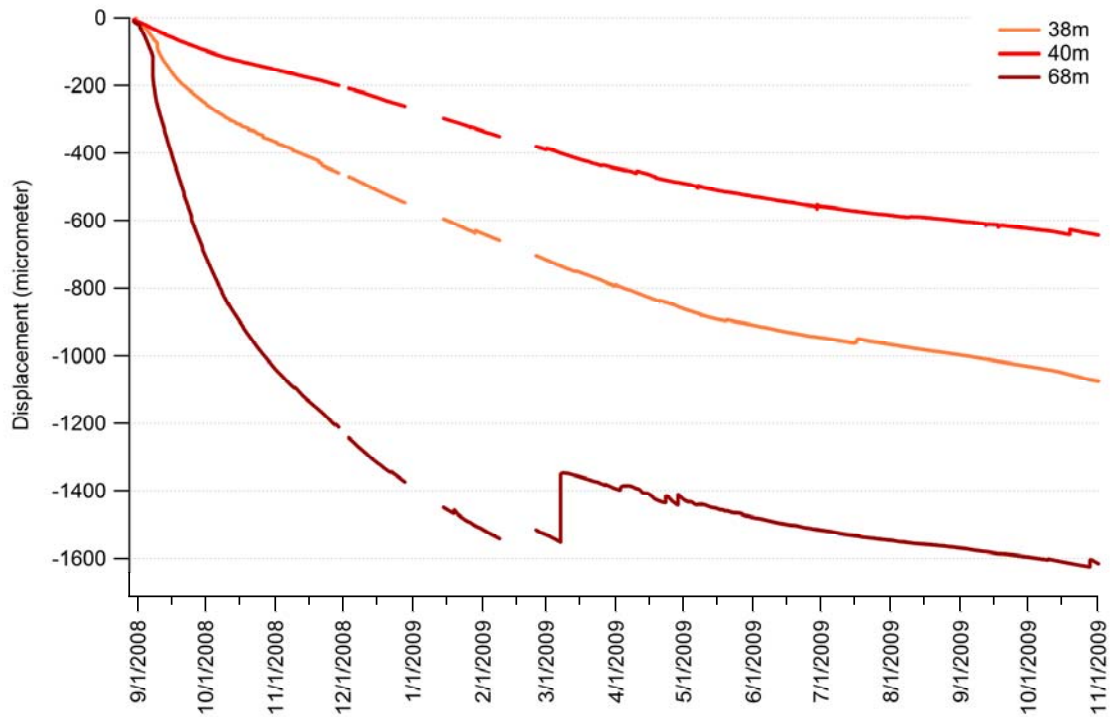


Figure 12: Fiber optic deformation time series for Randa borehole sb120 since installation. Figure reproduced from Moore et al., 2010.

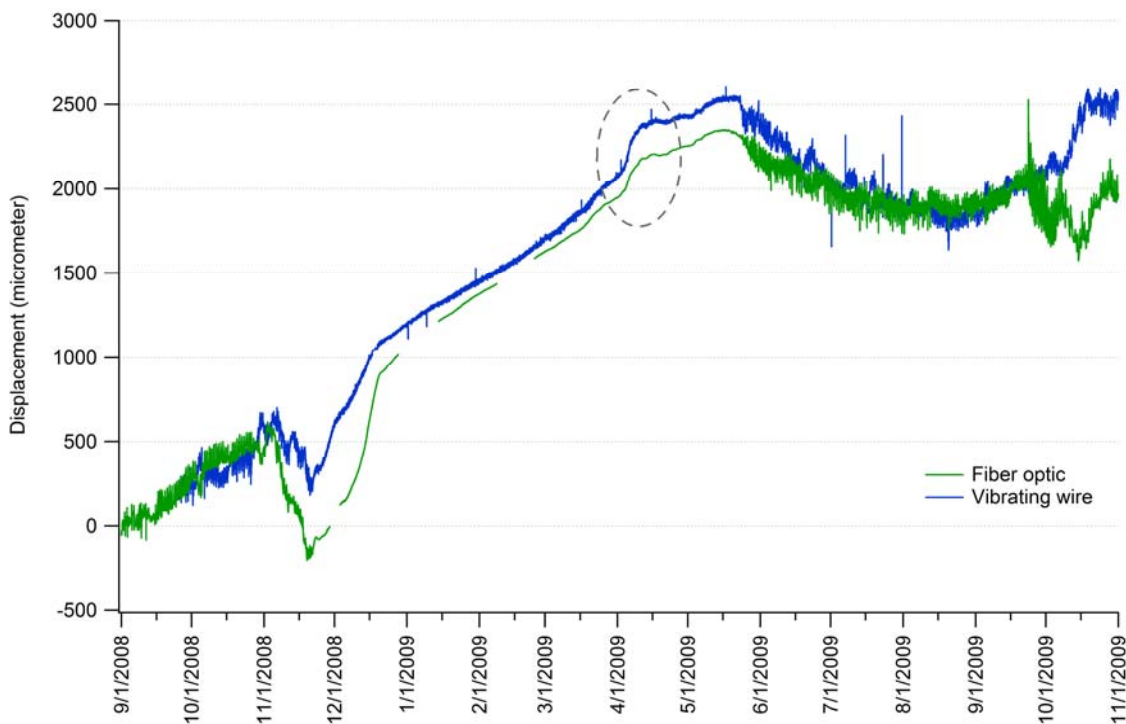


Figure 13: Fiber optic deformation time series for crack Z9 since installation, showing comparison with adjacent VW crackmeter. Figure reproduced from Moore et al., 2010.

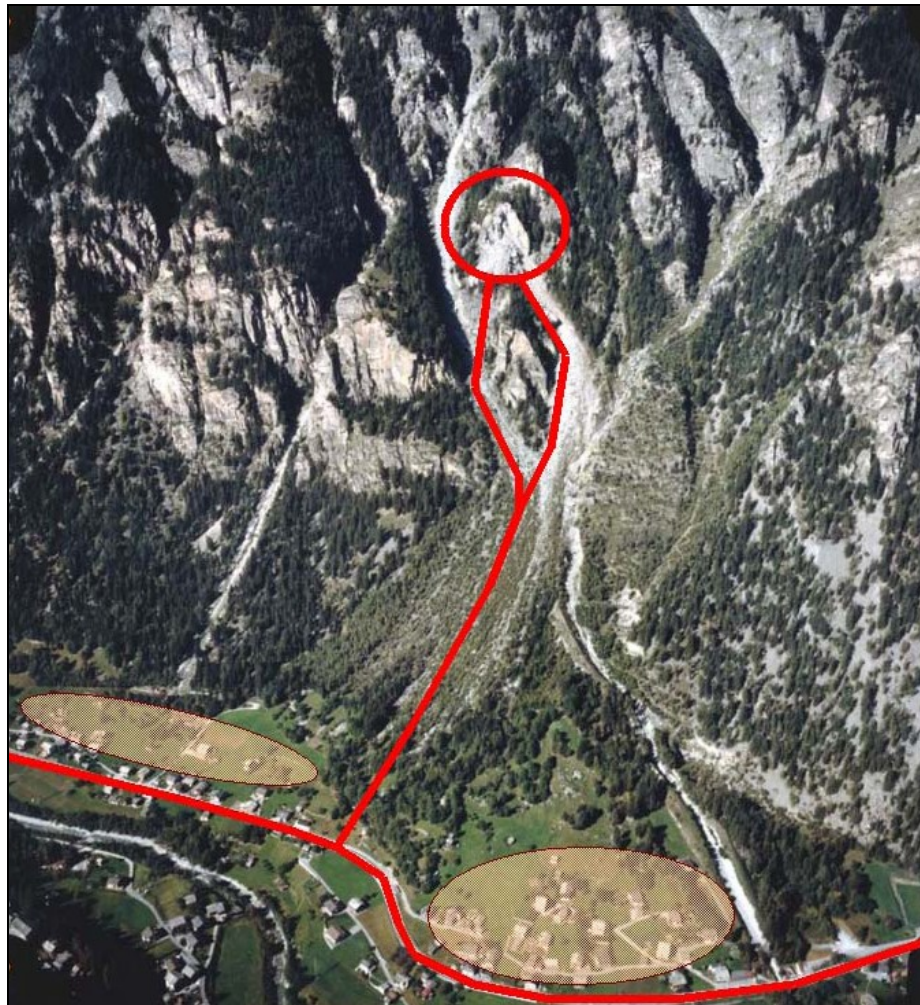
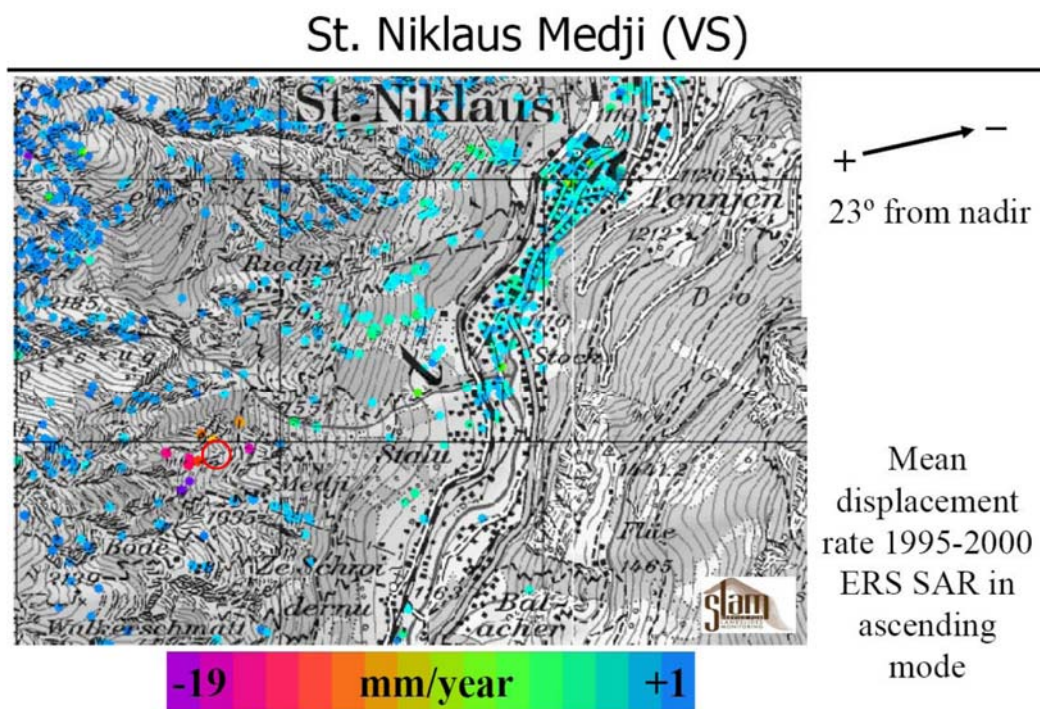


Figure 14: Overview of the Medji rockslide in 2002. The circled nose of rock collapsed, and the runout trace/s are shown. Endangered settlements are circled. Figure reproduced from Rovina + Partner AG, 2005.



Figure 15: The Medji rock slope in 2000 (left) and in 2002 (right). Figure reproduced from Joerg, 2008, modified from Rovina + partner, 2005.



J GAMMA REMOTE SENSING

Figure 16: Satellite In-SAR of the Medji rockslide area (circled) and surrounding rock slopes showing additional movement of nearby slopes. Figure courtesy of Gamma Remote Sensing, AG; see Joerg, 2008.

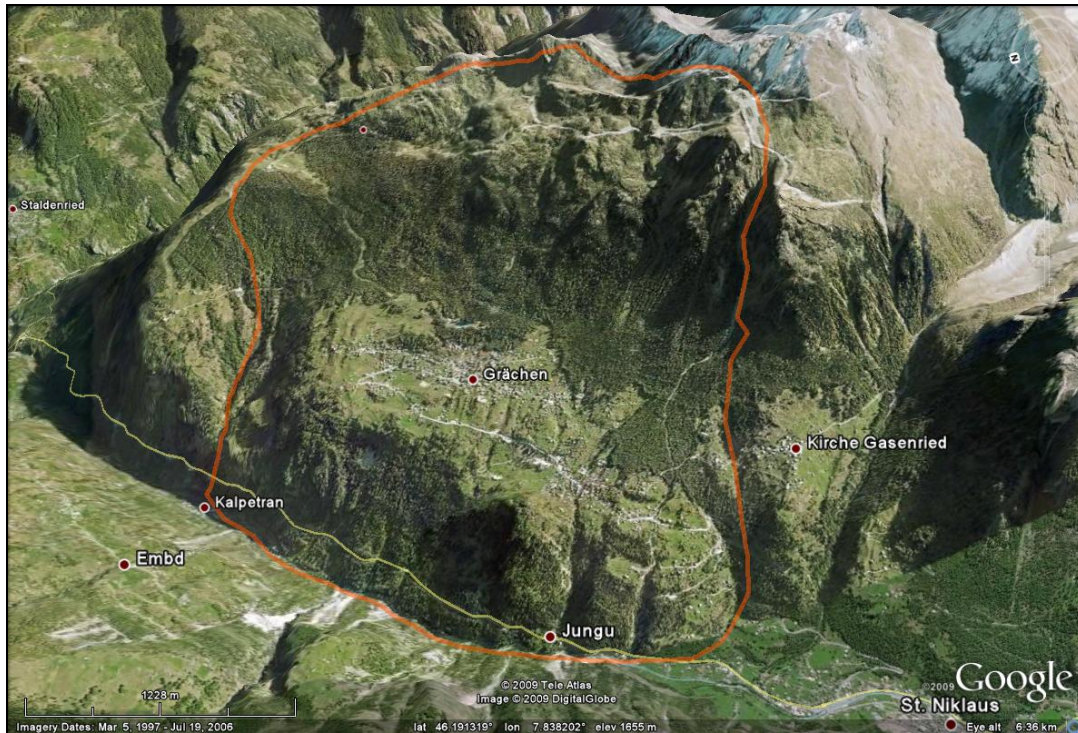


Figure 17: Graechen overview; approximate outline of the DSGSD is shown.



Figure 18: Graechen geodetic monitoring overview. Displacement vectors were calculated over a 62 year period from 1930-1992, and are scaled according to the legend in the lower left portion of the map. Figure reproduced from Noverraz et al. (1998).

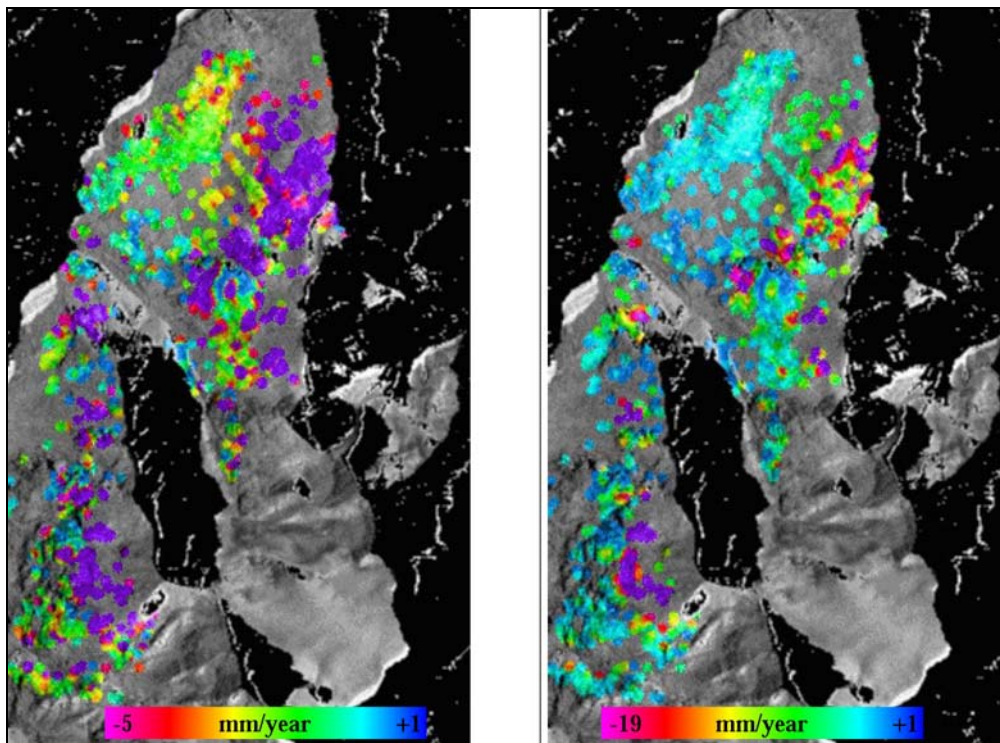


Figure 19: Overview of SLAM satellite interferometry displacement data at Graechen with two different color scales. Image reproduced from SLAM monographic report: Grächen, Montagnon & La Frasse (2004).

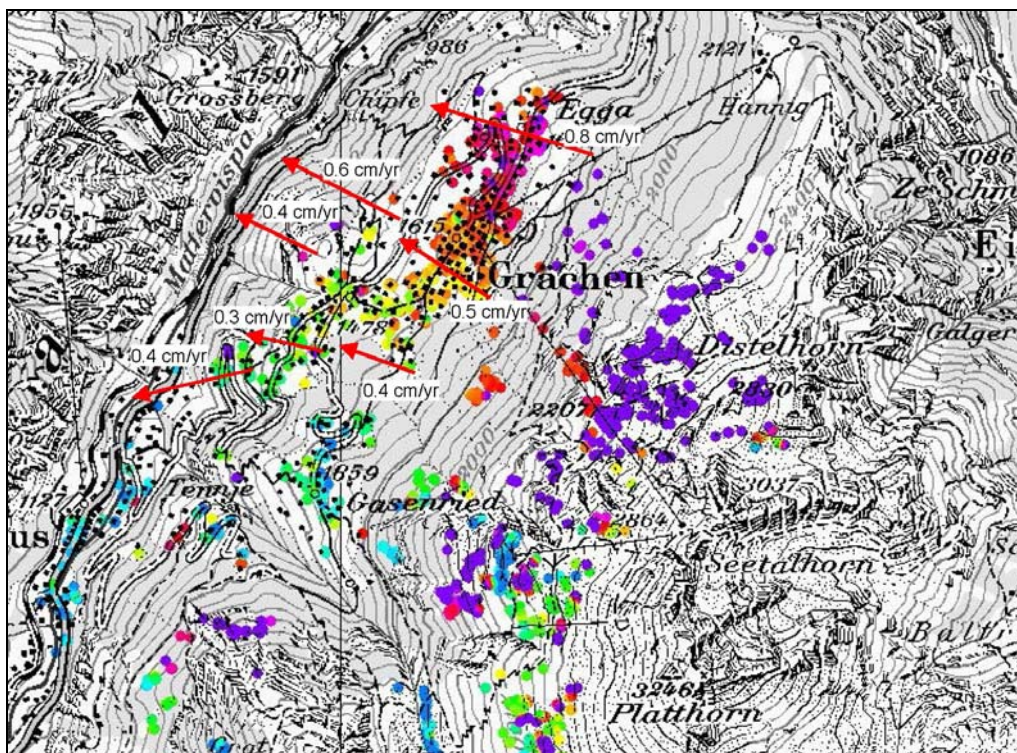


Figure 20: SLAM IPTA results compared to long-term geodetic measurements at Graechen. Figure reproduced from SLAM monographic report: Grächen, Montagnon & La Frasse (2004).



Figure 21: Overview of detail study sites at Graechen selected for time-lapse photography and laser scanning: Gabelhorn, Durlochhorn, and Platja.

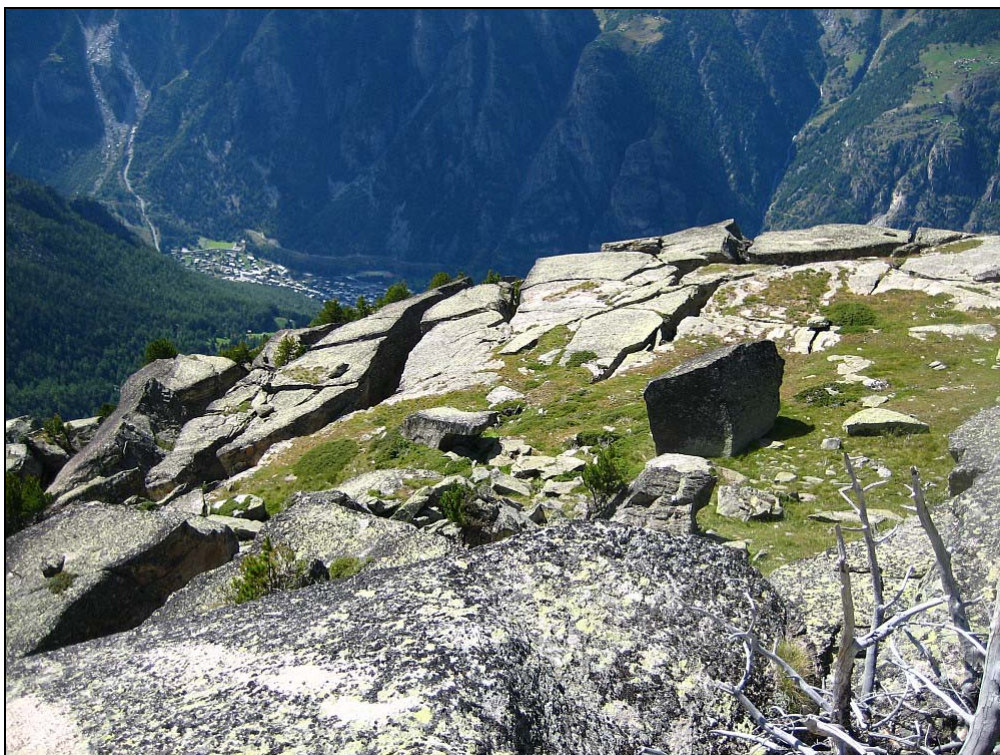


Figure 22: Detail of the Platja area showing large rock blocks separated by open cracks.

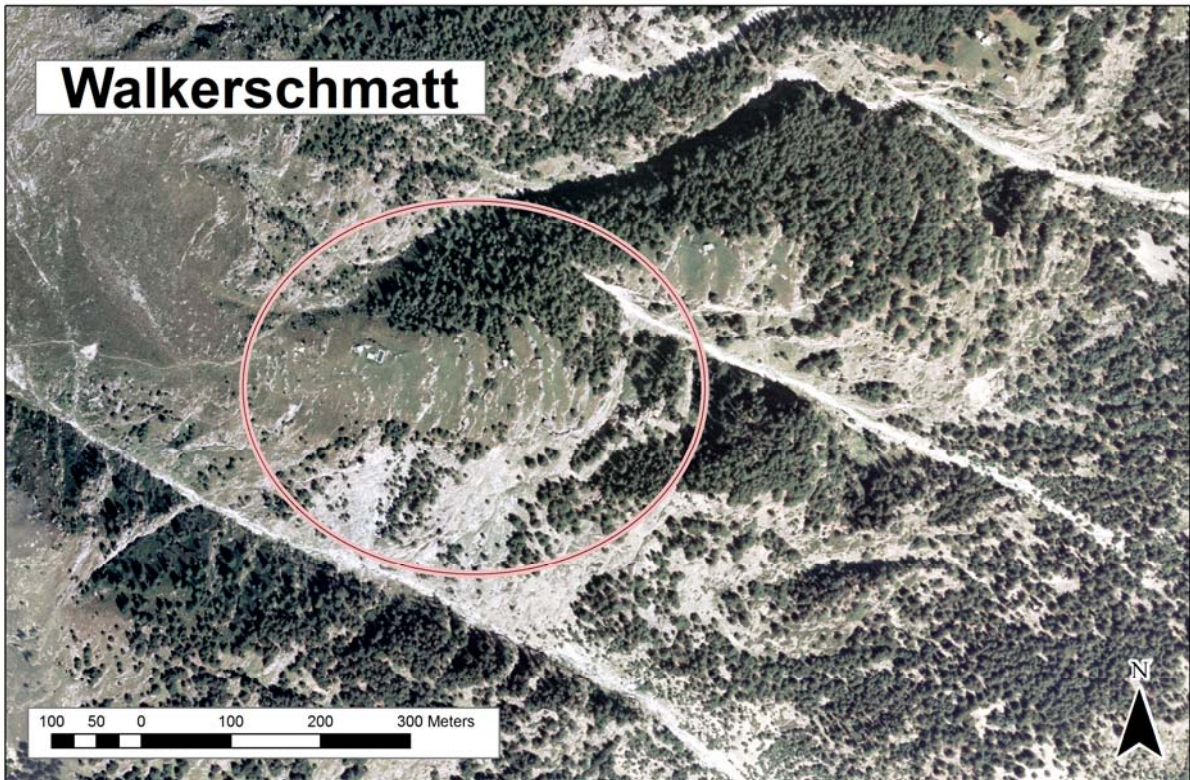


Figure 23: Overview of the Walkerschmatt area.

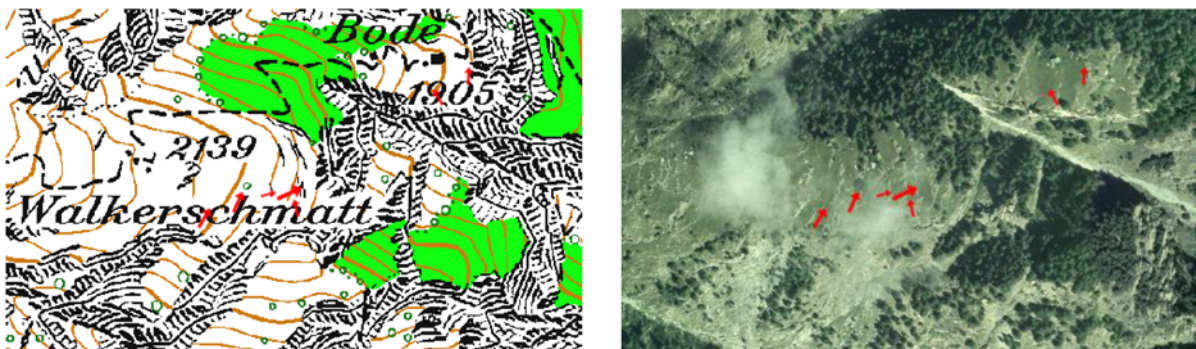


Figure 24: Precision differential GPS displacement measurements at Walkerschmatt. Arrows (five in total) are scaled by displacement magnitude; the three larger bold arrows are displacements above the computed accuracy level (though only slightly) and may be significant. Figure reproduced from Ingensand & Stempfhuber (2009).

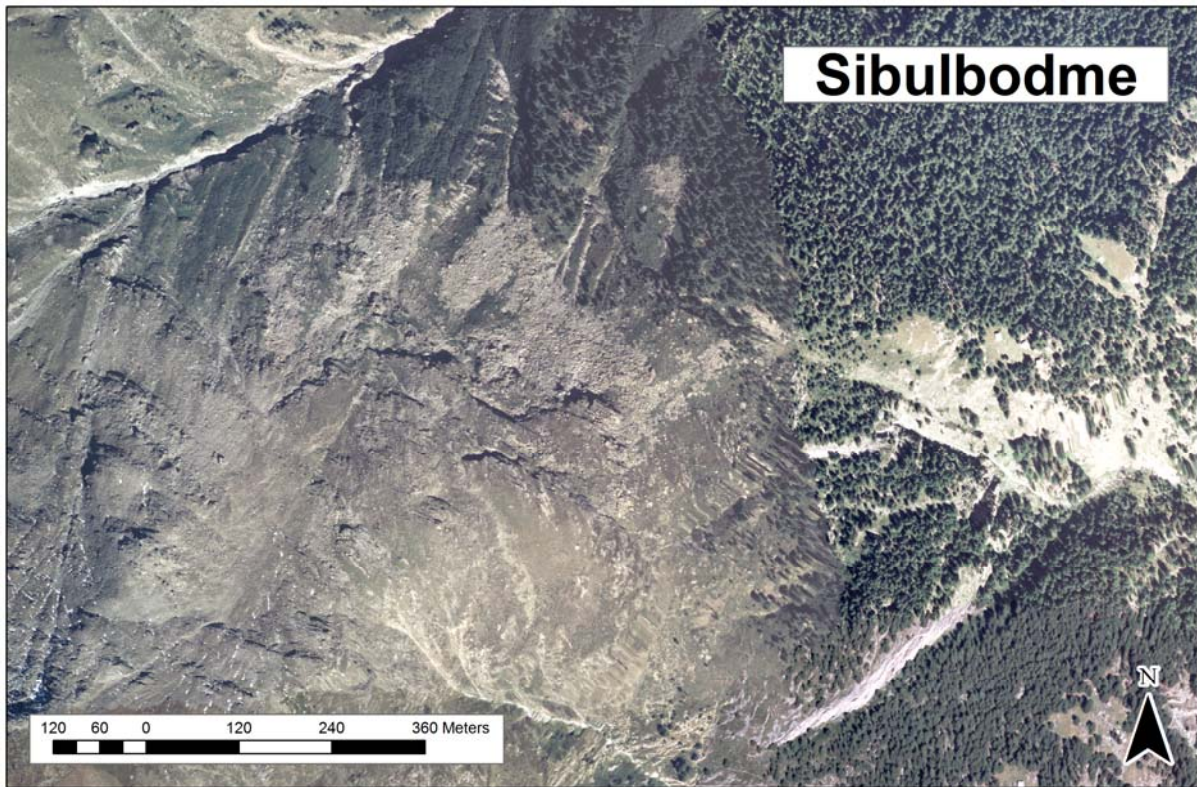


Figure 25: Overview of the Sibulbodme area.

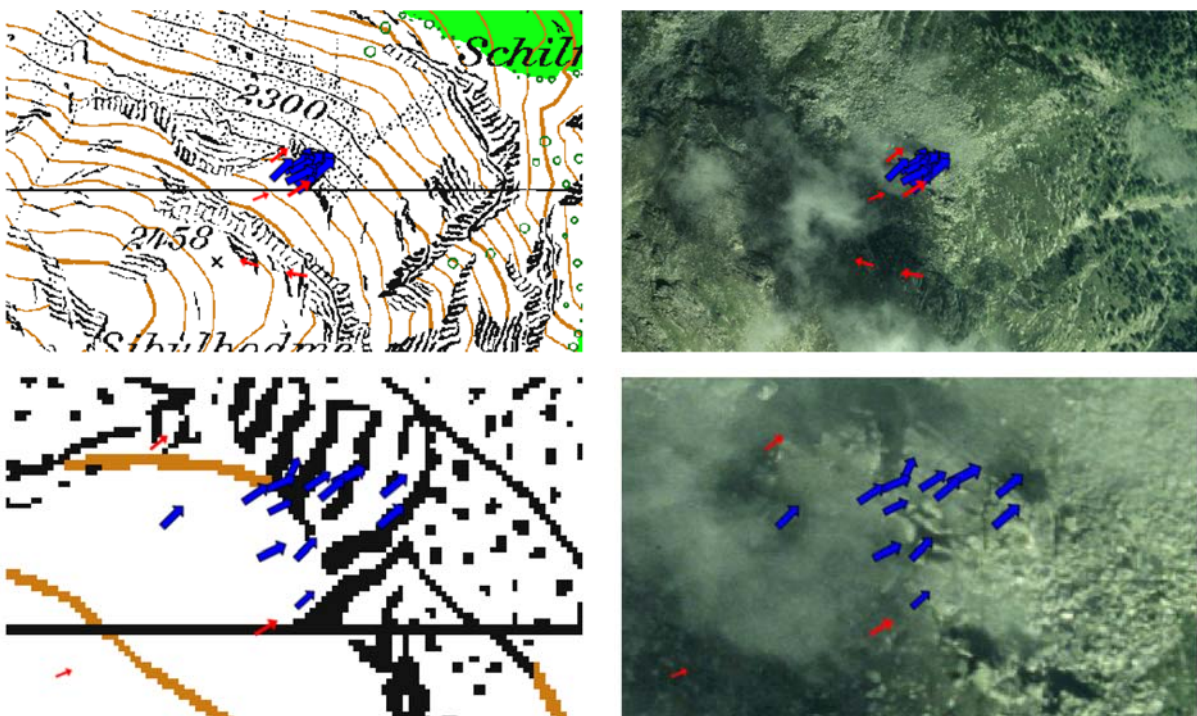


Figure 26: Precision GPS displacement measurements at Sibulbodme. Arrows are scaled by displacement magnitude. Red arrows are the fixed points, blue arrows are the local network. All blue arrows show displacements above the accuracy level and are therefore considered significant. Figure reproduced from Ingensand & Stempfhuber (2009).

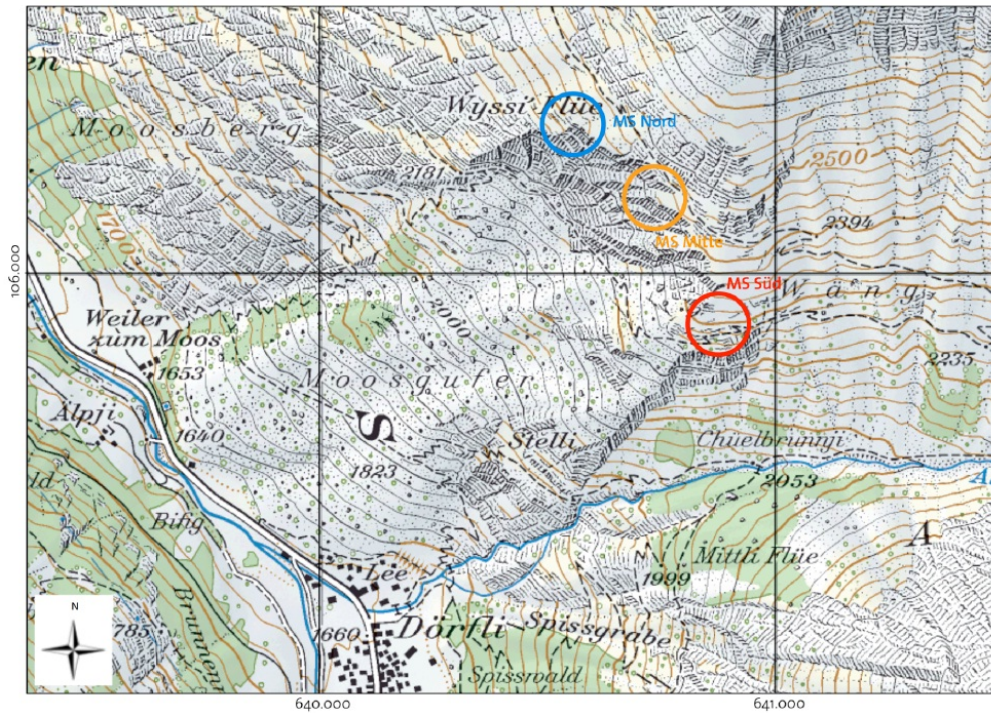


Figure 27: Overview of the Moosgufer rock slope failure and the location of the three in-situ measurement arrays.

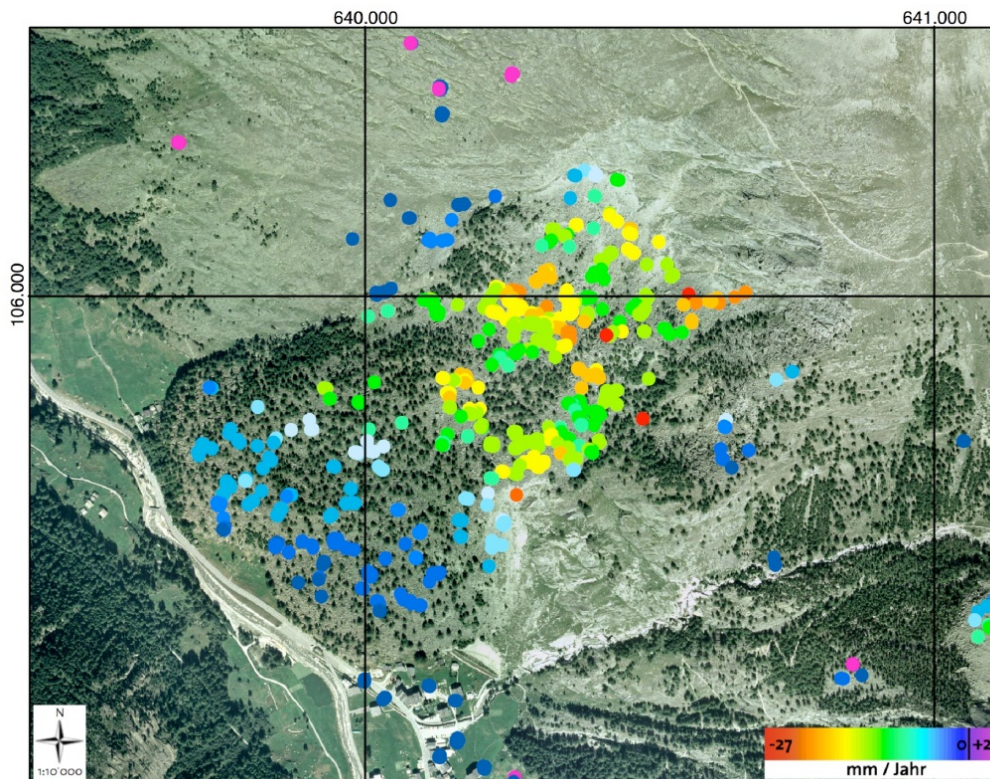


Figure 28: Satellite In-SAR IPTA points associated with the Moosgufer instability and surrounding rock slopes. Data reproduced from the SLAM Project with permission from the Swiss Federal Office for the Environment (BAFU), (Ruppen, 2009).